An Improved Model of Saturated Induction Machines

J. O. OJO, MEMBER, IEEE, ALFIO CONSOLI, SENIOR MEMBER, IEEE, AND THOMAS A. LIPO, FELLOW, IEEE

Abstract—**Conventional models of induction machines represent instantaneous saturation of the magnetizing flux by using either saturation factors or by adjusting the tangential and slope reactances. These models are often inaccurate in predicting states of the machine during transient conditions such as on-line starting. To remedy these inconsistencies, an improved equivalent circuit model is proposed that accounts not only for the saturation effects in the stator and rotor teeth but also, independently, for saturation in both the rotor and stator cores. The new model is compared with test results as well as with more conventional models. The new model demonstrates an improvement over other known models showing that detailed representations of saturation effects could be important in induction machine analysis, particularly when the machine is subjected to large signal disturbances.**

I. Introduction

THE PREDICTION of induction machine performance has traditionally been based on constant parameter models that have yielded good engineering results for both steady-state and most transient conditions [1]–[6]. However, the model has frequently not been sufficiently accurate for certain large signal transient conditions such as on-line starting. A perplexing problem concerning these conventional models is that while they may be accurate for predicting certain states of the machine such as inrush currents, they tend to give higher than measured electromagnetic torque. Since the electromagnetic torque is, in essence, the space vector product of stator current and air gap flux, this inconsistency casts doubt on the validity of conventional saturation models during such conditions. To remedy these inconsistencies, an improved equivalent circuit model is proposed that accounts not only for saturation in the stator and rotor cores but also, independently, for saturation effects in the stator and rotor teeth.

In the past, experimental difficulties encountered in the determination of the parameters of more detailed equivalent circuits have discouraged the use of a more detailed induction machine representation. However, this limitation has been removed with the advent of finite element methods which can now be used to calculate the necessary parameters for more advanced equivalent circuits. The modeling approach proposed in this paper combines the advantage of finite-element methods for parameter determination and the simplicity of the equivalent-circuit approach, making it attractive in terms of computational time compared to other advanced methods that solve the complete magnetic circuits at every time step [7].

With the aid of saturation factors obtained by means of finite-element methods and confirmed by tests, the equations of the induction machine in the arbitrary reference frame accounting for saturation effects in the stator and rotor cores and the stator and rotor teeth are derived. The model is used to predict the transient performance during a direct on line-start of an induction machine both with and without series compensation capacitors. The predicted results are compared with test results and with simulation results obtained from conventional models. The new model demonstrates an improvement over previous models showing that appropriate representation of the saturation effects in the stator and rotor cores and teeth is important in induction machine analysis particularly when the machine is subjected to large signal disturbances.

II. Induction Machine Equations Including Saturation Effects

The magnetomotive forces (MMF's) due to the currents flowing in the stator and rotor circuits give rise to flux linkages the components of which can be attributed as follows:

1) the leakage flux linkages in the stator and rotor end winding regions,
2) the slot leakage flux linkages of the windings placed in the stator and rotor slots,
3) the useful (air gap) flux linkages in the stator, rotor teeth, and in the air gap of the machine, and
4) the stator and rotor core flux linkages that are algebraic combinations of flux linkages in (2) and (3).

The magnetic paths through which the magnetomotive drops in the end-winding leakage paths, cores, the slot leakage paths, the stator and rotor teeth, and the air gap can be represented by reluctances as shown in Fig. 1(a). In this figure the reluctances corresponding to the stator and rotor core and stator and rotor teeth can be considered as saturable.

Paper IPCSD 89-9, approved by the Electric Machines Committee of the IEEE Industry Applications Society for presentation at the 1988 Industry Applications Society Annual Meeting, Pittsburgh, PA, October 2–7. Manuscript released for publication April 17, 1989. This work was supported in part by the Wisconsin Electric Machines and Power Electronics Consortium.

J. O. Ojo was with the Department of Electrical and Computer Engineering, University of Wisconsin, Madison, WI. He is now with the Electrical Engineering Department, Tennessee Technological University, P.O. Box 5004, Cookeville, TN 38505.

A. Consoli is with the Institute of Electrical Engineering, University of Catania, Viale Doria 6, Catania, Italy 95125.

T. A. Lipo is with the Department of Electrical and Computer Engineering, University of Wisconsin, 1415 Johnson Drive, Madison, WI 53706.

IEEE Log Number 8932116.

0093-9994/90/0300-0212$01.00

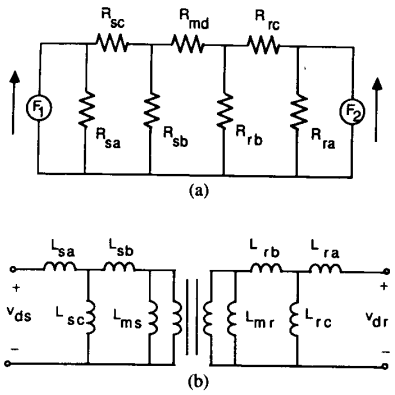

Fig. 1. Equivalent circuits of d axis flux component of induction machine. (a) Magnetic. (b) Electric.

Using the principles of topological duality, and the q-d transformation of winding distributions, the q-d electric equivalent circuits of the machine are as shown in Fig. 2 for the motoring convention. It is assumed here that the inductances representing the stator and rotor cores in addition to the magnetizing branch (representing the stator and rotor teeth as well as the air gap) are saturable. The possible saturation effects in the slot iron leakage paths will accounted for in the core saturation in this model.

The transient model for a machine having the per-phase magnetic equivalent circuit of Fig. 1(b) follows an approach similar to that of [3]. The voltage equations for the balanced three-phase squirrel-cage induction machine in the arbitrary reference frame are as follows:

$$v_{qs} = r_s i_{qs} + p\lambda_{qs} + \omega\lambda_{ds} \tag{1}$$

$$v_{ds} = r_s i_{ds} + p\lambda_{ds} - \omega\lambda_{qs} \tag{2}$$

$$v_{qr} = r_r i_{qr} + p\lambda_{qr} + (\omega - \omega_r)\lambda_{dr} \tag{3}$$

$$v_{dr} = r_r i_{dr} + p\lambda_{dr} - (\omega - \omega_r)\lambda_{qr}. \tag{4}$$

The equations for the flux linkages from the equivalent circuits are expressed in q-d variables by

$$\lambda_{qs} = L_{sa} i_{qs} + \lambda_{qsc}(\text{sat}) \tag{5}$$

$$\lambda_{ds} = L_{sa} i_{ds} + \lambda_{dsc}(\text{sat}) \tag{6}$$

$$\lambda_{qr} = L_{ra} i_{qr} + \lambda_{qrc}(\text{sat}) \tag{7}$$

$$\lambda_{dr} = L_{ra} i_{dr} + \lambda_{drc}(\text{sat}) \tag{8}$$

$$\lambda_{qsc} = L_{sb} i_{qss} + \lambda_{mq}(\text{sat}) \tag{9}$$

$$\lambda_{dsc} = L_{sb} i_{dss} + \lambda_{md}(\text{sat}) \tag{10}$$

$$\lambda_{qrc} = L_{rb} i_{qrr} + \lambda_{mq}(\text{sat}) \tag{11}$$

$$\lambda_{drc} = L_{rb} i_{drr} + \lambda_{md}(\text{sat}) \tag{12}$$

where

L_{sa}, L_{ra}	stator and rotor end-winding leakage inductances referred to the stator circuits, respectively;
L_{sc}, L_{rc}	stator and rotor core inductances referred to the stator circuits, respectively;
L_{sb}, L_{rb}	stator and rotor slot leakage inductances referred to the stator circuits, respectively;
ω	speed of the arbitrary reference frame;
p	$=d/dt$;
$\lambda_{qs}, \lambda_{ds}$	q and d stator total flux linkages, respectively;
$\lambda_{qr}, \lambda_{dr}$	q and d rotor total flux linkages, respectively;
$\lambda_{qrc}, \lambda_{drc}$	q and d rotor core flux linkages, respectively;
$\lambda_{qsc}, \lambda_{dsc}$	q and d stator core flux linkages, respectively;
$\lambda_{mq}, \lambda_{md}$	q and d magnetizing flux linkages, respectively.

The currents are given by

$$i_{qs} = [\psi_{qs} - \psi_{qsc}(\text{sat})]/X_{sa} \tag{13}$$

$$i_{ds} = [\psi_{ds} - \psi_{dsc}(\text{sat})]/X_{sa} \tag{14}$$

$$i_{qr} = [\psi_{qr} - \psi_{qrc}(\text{sat})]/X_{ra} \tag{15}$$

$$i_{dr} = [\psi_{dr} - \psi_{drc}(\text{sat})]/X_{ra} \tag{16}$$

$$i_{qss} = [\psi_{qsc}(\text{sat}) - \psi_{mq}(\text{sat})]/X_{sb} \tag{17}$$

$$i_{dss} = [\psi_{dsc}(\text{sat}) - \psi_{md}(\text{sat})]/X_{sb} \tag{18}$$

$$i_{qrr} = [\psi_{qrc}(\text{sat}) - \psi_{mq}(\text{sat})]/X_{rb} \tag{19}$$

$$i_{drr} = [\psi_{drc}(\text{sat}) - \psi_{md}(\text{sat})]/X_{rb} \tag{20}$$

where in (13)-(20) the inductances have been replaced by equivalent reactances, i.e., $X_{sa} = \omega_b L_{sa}$, and where ω_b is the base reference angular velocity. Similarly, the flux linkages λ has been replaced by a modified flux linkage ψ having units of flux linkages per second or volts, i.e., $\psi_{qs} = \omega_b \lambda_{qs}$. In (13)-(20),

i_{qs}, i_{ds}	q and d currents flowing into the stator terminals,
i_{qss}, i_{dss}	q and d currents flowing into the magnetizing branch from the stator,
i_{qr}, i_{dr}	q and d currents flowing into the rotor circuit from the rotor terminal,
i_{qrr}, i_{drr}	q and d current flowing into the magnetizing branch from the rotor.

The unsaturated magnetizing flux in the d and q axis is given as

$$\lambda_{mq}(\text{unsat}) = L_m(i_{qrr} + i_{qss}) \tag{21}$$

$$\lambda_{md}(\text{unsat}) = L_m(i_{drr} + i_{dss}) \tag{22}$$

L_m	magnetizing inductance which represents the combined reluctances of the stator, rotor teeth, and the air gap.

The equations for current (13)–(16) are substituted into (1)–(4) to obtain the following flux linkage equations:

$$\frac{p}{\omega_b}\psi_{qs} = v_{qs} + \frac{r_s}{X_{sa}}(\psi_{qsc}(\text{sat}) - \psi_{qs}) - \frac{\omega}{\omega_b}\psi_{dss} \quad (23)$$

$$\frac{p}{\omega_b}\psi_{ds} = v_{ds} + \frac{r_s}{X_{sa}}(\psi_{dsc}(\text{sat}) - \psi_{ds}) + \frac{\omega}{\omega_b}\psi_{qs} \quad (24)$$

$$\frac{p}{\omega_b}\psi_{qr} = v_{dr} + \frac{r_r}{X_{sa}}(\psi_{qrc}(\text{sat}) - \psi_{qr}) - \frac{1}{\omega_b}(\omega - \omega_r)\psi_{dr} \quad (25)$$

$$\frac{p}{\omega_b}\psi_{dr} = v_{qr} + \frac{r_r}{X_{sa}}(\psi_{drc}(\text{sat}) - \psi_{dr}) + \frac{1}{\omega_b}(\omega - \omega_r)\psi_{qr}. \quad (26)$$

The computation of the saturated flux linkages must now be considered. For this purpose the method of saturation factors can be employed [1], [3]. The saturated q–d fluxes linkages in the magnetizing branch can be expressed:

$$\psi_{mq}(\text{sat}) = \psi_{mq}(\text{unsat}) - \Delta\psi_{mq} \quad (27)$$

$$\psi_{md}(\text{sat}) = \psi_{md}(\text{unsat}) - \Delta\psi_{md}. \quad (28)$$

The changes in magnetizing fux linkages due to saturation are now given as follows:

$$\Delta\psi_{mq} = (1 - K_m)\psi_{mq}(\text{unsat}) \quad (29)$$

$$\Delta\psi_{md} = (1 - K_m)\psi_{md}(\text{unsat}) \quad (30)$$

where K_m is the saturation factor which is a function of the resultant unsaturated magnetizing flux given as

$$\psi_m(\text{unsat}) = \sqrt{[\psi_{mq}^2(\text{unsat}) + \psi_{md}^2(\text{unsat})]} \quad (31)$$

and $\Delta\psi_{mq}$ and $\Delta\psi_{md}$ are the changes in the flux linkage levels from the unsaturated value in the q and d axis respectively.

When the expressions for current in (17)–(20) are substituted in (21) and (22), the following equations are obtained:

$$\psi_{mq}(\text{unsat}) = \frac{X_{mm}}{X_{sb}}\psi_{qsc}(\text{sat}) + \frac{X_{mm}}{X_{rb}}\psi_{qrc}(\text{sat}) + X_{mm}\left[\frac{1}{X_{rb}} + \frac{1}{X_{sb}}\right]\Delta\psi_{mq} \quad (32)$$

$$\psi_{md}(\text{unsat}) = \frac{X_{mm}}{X_{sb}}\psi_{dsc}(\text{sat}) + \frac{X_{mm}}{X_{rb}}\psi_{drc}(\text{sat}) + X_{mm}\left[\frac{1}{X_{rb}} + \frac{1}{X_{sb}}\right]\Delta\psi_{md} \quad (33)$$

where

$$X_{mm} = 1/\left(\frac{1}{X_m} + \frac{1}{X_{sb}} + \frac{1}{X_{rb}}\right). \quad (34)$$

The unsaturated core fluxes linkages in volts are related to currents by

$$\psi_{qsc}(\text{unsat}) = X_{sc}(i_{qs} - i_{qss}) \quad (35)$$

$$\psi_{dsc}(\text{unsat}) = X_{sc}(i_{ds} - i_{dss}) \quad (36)$$

$$\psi_{qrc}(\text{unsat}) = X_{rc}(i_{qr} - i_{qrr}) \quad (37)$$

$$\psi_{drc}(\text{unsat}) = X_{rc}(i_{dr} - i_{drr}). \quad (38)$$

In a similar manner as for the magnetizing flux linkage component, the changes in the core flux linkages due to saturation are

$$\Delta\psi_{qsc} = (1 - K_s)\psi_{qsc}(\text{unsat}) \quad (39)$$

$$\Delta\psi_{dsc} = (1 - K_s)\psi_{dsc}(\text{unsat}) \quad (40)$$

$$\Delta\psi_{qrc} = (1 - K_r)\psi_{qrc}(\text{unsat}) \quad (41)$$

$$\Delta\psi_{drc} = (1 - K_r)\psi_{drc}(\text{unsat}). \quad (42)$$

The saturated q–d core fluxes are given as

$$\psi_{qsc}(\text{sat}) = \psi_{qsc}(\text{unsat}) - \Delta\psi_{qsc} \quad (43)$$

$$\psi_{dsc}(\text{sat}) = \psi_{dsc}(\text{unsat}) - \Delta\psi_{dsc} \quad (44)$$

$$\psi_{qrc}(\text{sat}) = \psi_{qrc}(\text{unsat}) - \Delta\psi_{qrc} \quad (45)$$

$$\psi_{drc}(\text{sat}) = \psi_{drc}(\text{unsat}) - \Delta\psi_{drc} \quad (46)$$

where $\Delta\psi_{qsc}$ and $\Delta\psi_{dsc}$ are the changes in the d and q components of stator core fluxes due to saturation of the stator core and $\Delta\psi_{qrc}$ and $\Delta\psi_{drc}$ are the changes in the rotor fluxes in the q and d axes due to saturation in the rotor core.

The quantities K_s and K_r are the saturation factors for the stator and rotor cores as functions of the unsaturated stator and rotor fluxes, respectively. The unsaturated stator and rotor core fluxes are given respectively as

$$\psi_{sc}(\text{unsat}) = \sqrt{[\psi_{qsc}^2(\text{unsat}) + \psi_{dsc}^2(\text{unsat})]} \quad (47)$$

$$\psi_{rc}(\text{unsat}) = \sqrt{[\psi_{qrc}^2(\text{unsat}) + \psi_{drc}^2(\text{unsat})]} \quad (48)$$

Substituting for the currents, the core flux linkages in volts can be written as

$$\psi_{qsc}(\text{unsat}) = X_{scc}\left[\frac{\psi_{qs}}{X_{sa}} + \frac{\psi_{mq}}{X_{sb}}(\text{sat})\right] + X_{scc}\left[\frac{1}{X_{sa}} + \frac{1}{X_{sb}}\right]\Delta\psi_{qsc} \quad (49)$$

$$\psi_{dsc}(\text{unsat}) = X_{scc}\left[\frac{\psi_{ds}}{X_{sa}} + \frac{\psi_{md}}{X_{sb}}(\text{sat})\right] + X_{scc}\left[\frac{1}{X_{sa}} + \frac{1}{X_{sb}}\right]\Delta\psi_{dsc} \quad (50)$$

$$\psi_{qrc}(\text{unsat}) = X_{rcc}\left[\frac{\psi_{qr}}{X_{ra}} + \frac{\psi_{mq}}{X_{rb}}(\text{sat})\right] + X_{rcc}\left[\frac{1}{X_{ra}} + \frac{1}{X_{rb}}\right]\Delta\psi_{qrc} \quad (51)$$

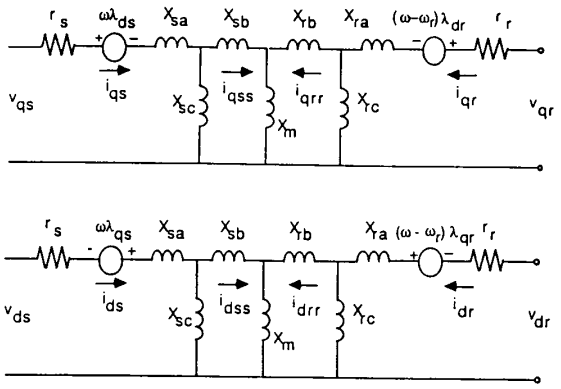

Fig. 2. *d-q* equivalent circuit model of induction machine.

$$\psi_{drc}(\text{unsat}) = X_{rcc}\left[\frac{\psi_{dr}}{X_{ra}} + \frac{\psi_{md}}{X_{rb}}(\text{sat})\right] + X_{rcc}\left[\frac{1}{X_{ra}} + \frac{1}{X_{rb}}\right]\Delta\psi_{drc} \quad (52)$$

where

$$X_{scc} = 1\Big/\left(\frac{1}{X_{sc}} + \frac{1}{X_{sa}} + \frac{1}{X_{sb}}\right) \quad (53)$$

$$X_{rcc} = 1\Big/\left(\frac{1}{X_{rc}} + \frac{1}{X_{ra}} + \frac{1}{X_{rb}}\right). \quad (54)$$

Finally, the equation for the electromagnetic torque for the saturated induction machine and the equation of motion can be written in the conventional form:

$$T_e = \frac{3}{2}\frac{P}{2}(\lambda_{ds}i_{qs} - \lambda_{qs}i_{ds}) \quad (55)$$

$$J\frac{d\omega_r}{dt} = T_e - T_1. \quad (56)$$

Equations (23)–(56) form the basis for the computer simulation of an induction machine that incorporates independent saturation in the stator core, rotor core, and magnetizing branch.

III. Determination of Machine Parameters and Saturation Factors

To implement the proposed model, a method for the determination of the nonconventional parameters was devised. In particular, the test machine was mechanized with search coils in the air gap, the stator slot, and around the stator core for the measurement of induced voltages under varying load and terminal voltage conditions. The measured induced voltages and measured terminal currents were used to calculate the stator core, slot leakage, magnetizing reactances and their corresponding saturation factors for varying degrees of excitation. Finite element methods were also used to compute these parameters and to correlate with the tested values.

Figs. 3 and 4 show, respectively, the stator core flux and magnetizing flux saturation factors for the test machine obtained both by tests and by the finite element method. Good correlations were obtained between the saturation factors obtained by the two methods. It was determined that the rotor core of the test machine was essentially unsaturated under all reasonable operating conditions so that only two saturation functions were ultimately used to correlate with tested results. Since the experimental approach to determine the parameters of the machine is tedious and involved, it is suggested that in the future the finite element method be used to compute the machine parameters and saturation factors when the machine geometries are known.

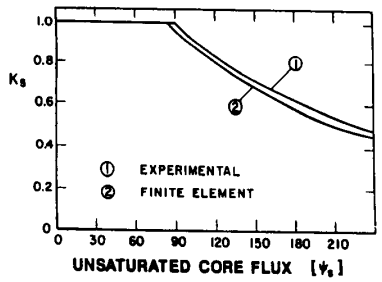

Fig. 3. Saturation factor for stator core as function of total unsaturated core flux.

IV. Experimental Verification of Saturation Models

The model proposed in this paper has been compared to test results as well as to two other circuit models. One of these models is the constant parameter model whose parameters are fixed at values corresponding to rated voltage and rated load. The second model accounts for saturation effects in the magnetizing branch and also the slot leakage paths using saturation factors [3]. Using the machine whose parameters are shown in the Appendix, the starting transient performance for direct on line starting with and without and the series compensating capacitors have been simulated for the three models.

Figs. 5–8 show the results of the computed and measured performance for a direct on-line start of the induction machine. Fig. 5 gives the starting phase *a* current, which indicates that the model accounting for saturation in the stator core gives better correlation to the measured results. The current predicted by this model is a little greater than the current predicted from the constant parameter model and *a* slightly less than that predicted by the model accounting for saturation effects in the magnetizing branch and stator leakage paths. The significant difference is at the steady state where the current predicted by the new model is greater than that of the constant parameter model due to the increased influence of saturation in the stator core and magnetizing branch.

Fig. 6 portrays the developed electromagnetic torque of the machine. It can be seen that the model accounting for saturation in the stator core and magnetizing branch predicts a lesser torque than that predicted by the constant-parameter model and the model accounting for saturation in the slot leakage and magnetizing paths. The latter model clearly overestimates the developed electromagnetic torque even though it gave good prediction for the starting current. Although the developed torque has not been measured, experience shows that the actual measured developed torque is generally less than computed values using the constant parameter model, a trend that is seen in Fig. 6.

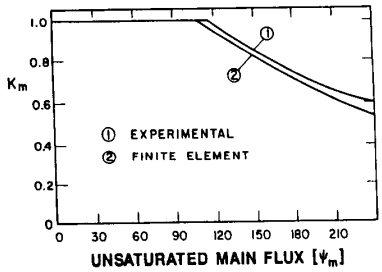

Fig. 4. Saturation factor for magnetizing main flux as function of unsaturated total main flux.

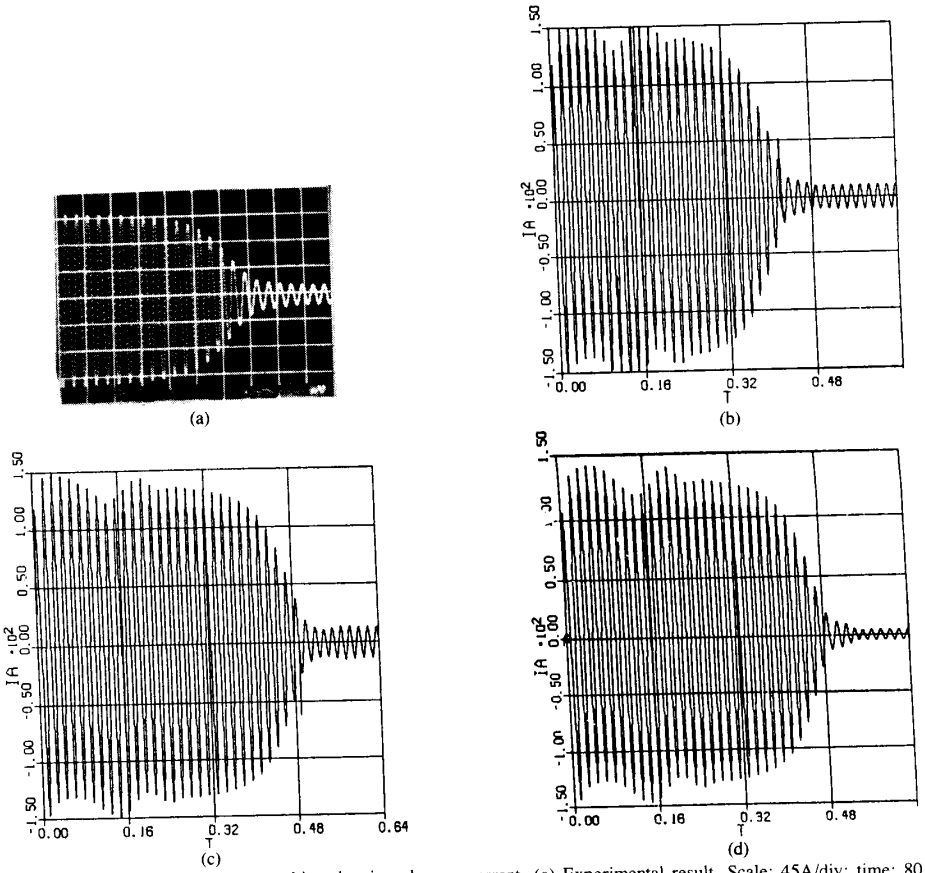

Fig. 5. Starting transient of induction machine showing phase *a* current. (a) Experimental result. Scale: 45A/div; time: 80 ms/div. (b) Model with saturation in stator core and magnetizing main flux paths. (c) Model with saturation in slot leakage and magnetizing main flux paths. (d) Constant parameter model.

Fig. 7 shows the computed and measured runup speed of the machine. The time taken to reach steady state is very much the same, and the difference in these cases are not of great practical importance. Nevertheless, the model accounting for the saturation effects in the magnetizing branch and the stator slot leakage paths gives (incorrectly) the least runup time because it has the least value of stator leakage reactance on starting. The simulation and test results show that saturation plays an important part in predicting starting torque in an inductance machine even though the flux in the air gap is only a fraction of the rated value. In this case saturation occurs due to core flux which is not normally considered saturable in the conventional *d–q* equivalent circuit.

The influence of saturation effects are seen most convincingly in the damping of electrical transients. In particular, it appears that saturation is particularly important in situations where the machine has nearly zero damping since the added damping introduced by saturation has a major influence on whether the machine is ultimately stable or unstable. Since small differences in saturation have a noticeable effect on the stability margin, the starting of an induction machine connected to the supply compensated with series capacitors. The condition was chosen to verify further the accuracy of the improved model. Series capacitance values corresponding to successful starting were chosen for the simulation and experiment. Figs. 8–11 show the performance of the machine un-

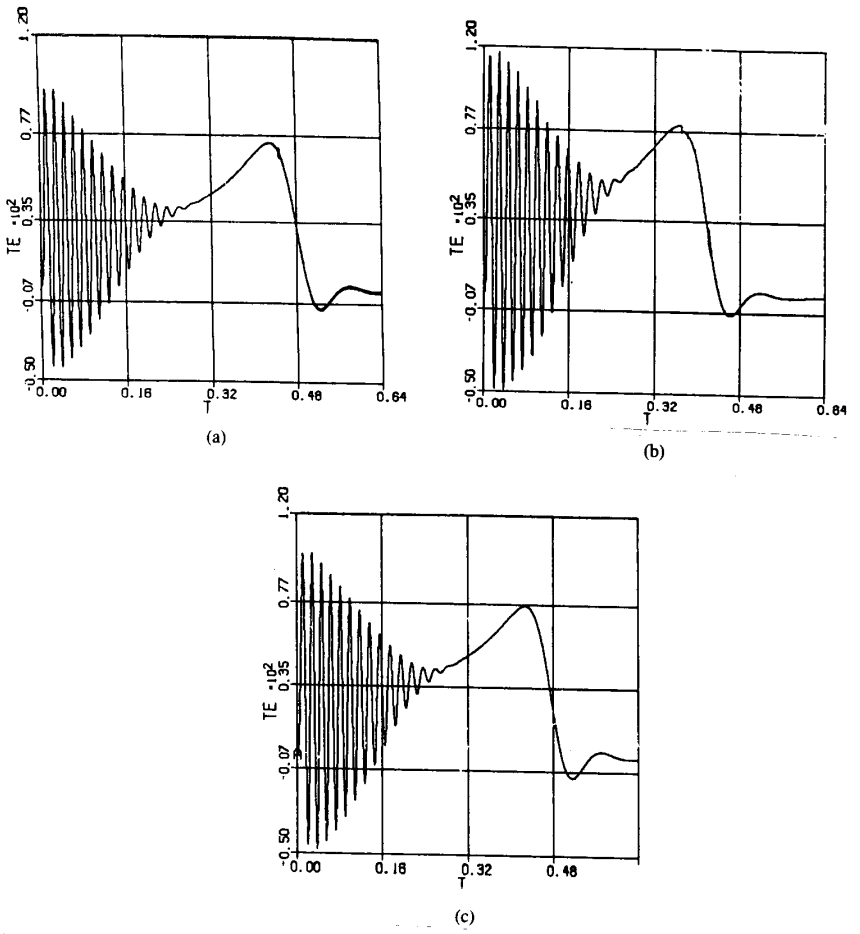

Fig. 6. Starting transient of induction machine showing developed electromagnetic torque. (a) Model with saturation in stator core and magnetizing main flux paths. (b) Model with saturation in slot leakage and magnetizing main flux paths. (c) Constant parameter model.

der this operating condition. It is seen that while the machine had a successful start and attained rated steady-state speed, the constant parameter model and the model that accounts for saturation in the magnetizing branch and slot leakage path predicted that the machine lapses into subsynchronous resonance. The improved model, however, gave a prediction that is very close to test results. The improved model predicts that the machine will achieve rated speed operation and has some oscillations in the steady-state currents and developed torque which are also evident in the test results. In this case it is quite apparent that the model accounting for saturation in the magnetizing branch and stator leakage paths yields better predictions than the constant parameter model.

V. Conclusion

The saturation effects of the both the stator and rotor core and teeth play an important role in the transient as well as dynamic performance of the induction machine. It has been shown that including both stator core and main flux (i.e., tooth) saturation significantly affects the damping of electrical transients and increases the accuracy of large transient performance prediction. This model clearly requires advanced measurement and/or finite-element computations for calculation of the equivalent circuit parameters. However, the model should be considered for abnormal conditions in which conventional models fail. The model proposed in this paper should also prove useful in improved computation of the iron losses of induction machines, a component of loss which plays an important role in the design optimization of high-efficiency machines.

Appendix I

Parameters of Test Induction Motor

The machine rating is 7.5 hp, 230/460 V, 20A rated current:

- stator resistance per phase $r_s = 0.2069\ \Omega$
- rotor resistance per phase $r_r = 0.298\ \Omega$
- stator end winding reactance per phase $X_{sa} = 0.242\ \Omega$
- stator slot leakage reactance per phase, $X_{sb} = 0.325\ \Omega$

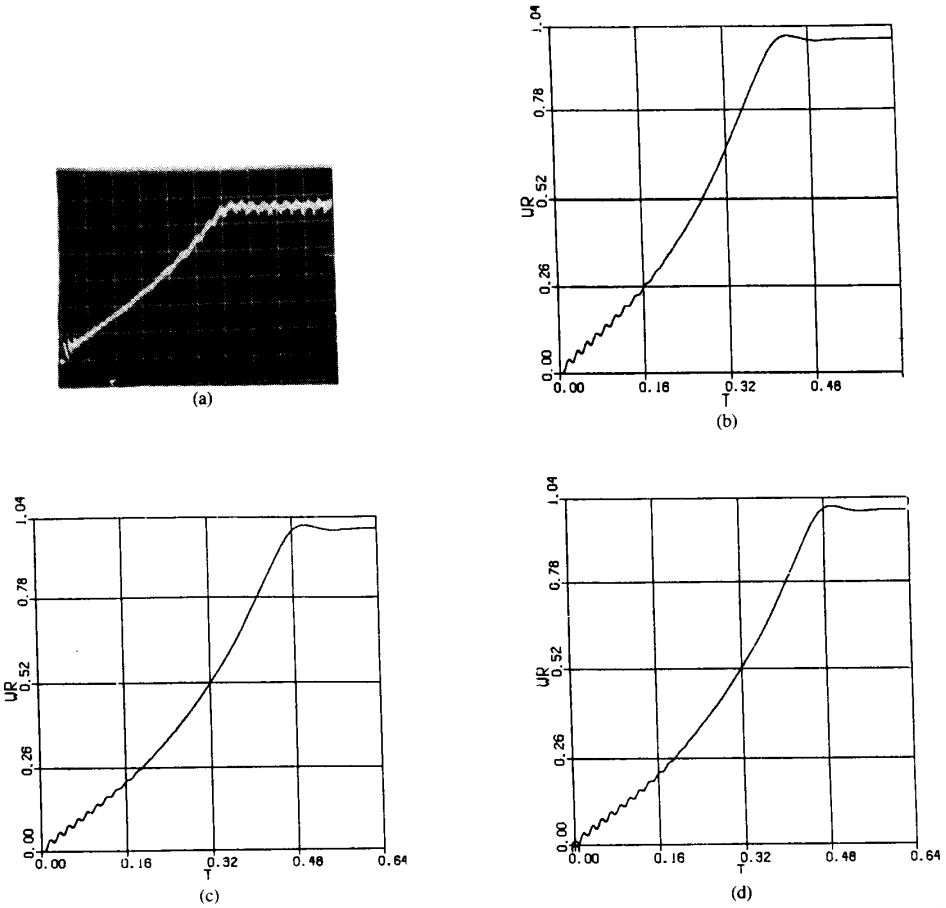

Fig. 7. Starting transient of induction machine showing speed run up. (a) Experimental result. Scale: time 80 ms/div. (b) Model with saturation in stator core and magnetizing main flux paths. (c) Model with saturation in slot leakage and magnetizing main flux paths. (d) Constant parameter model.

Fig. 8. Starting performance of induction machine fed by series compensated lines. Experimental results. (a) Stator phase *a* current. Scale: 25 A/div. (b) Runup speed in per unit.

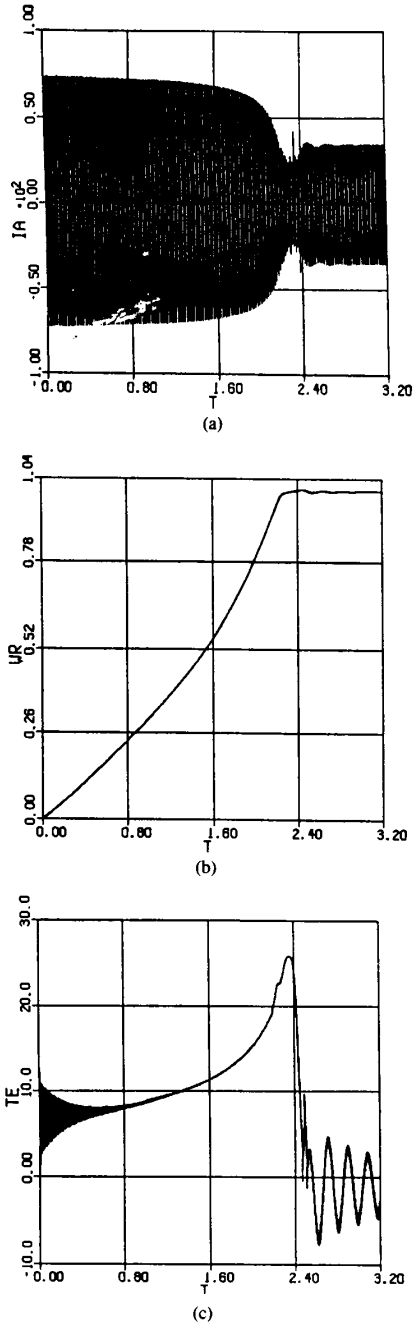

Fig. 9. Starting performance of induction machine fed by series compensated lines. Model with saturation in stator core and magnetizing main flux paths. (a) Stator phase *a* current. (b) Runup speed in per unit. (c) Developed electromagnetic torque.

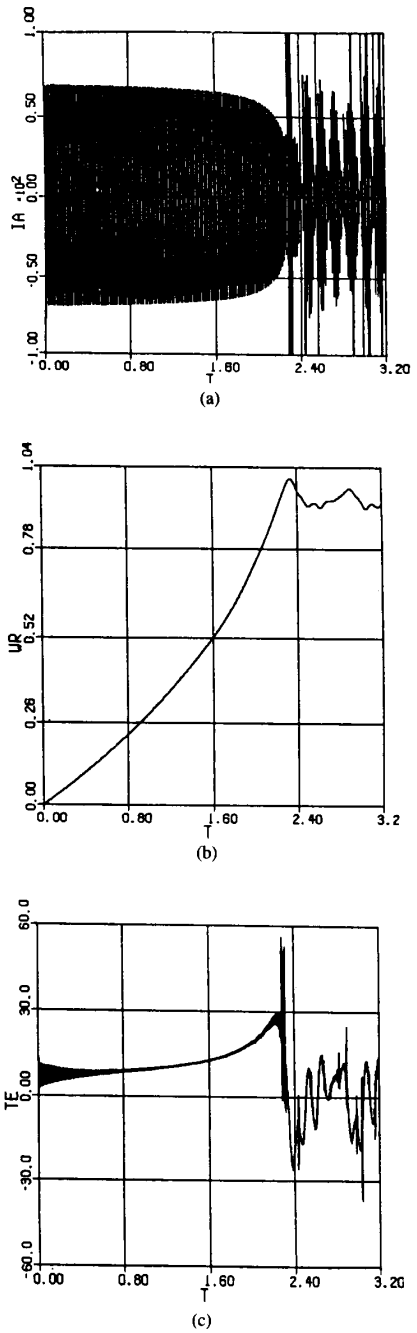

Fig. 10. Starting performance of induction machine fed by series compensated lines. Model with saturation in slot leakage and magnetizing main flux paths. (a) Stator phase *a* current. (b) Runup speed in per unit. (c) Developed electromagnetic torque.

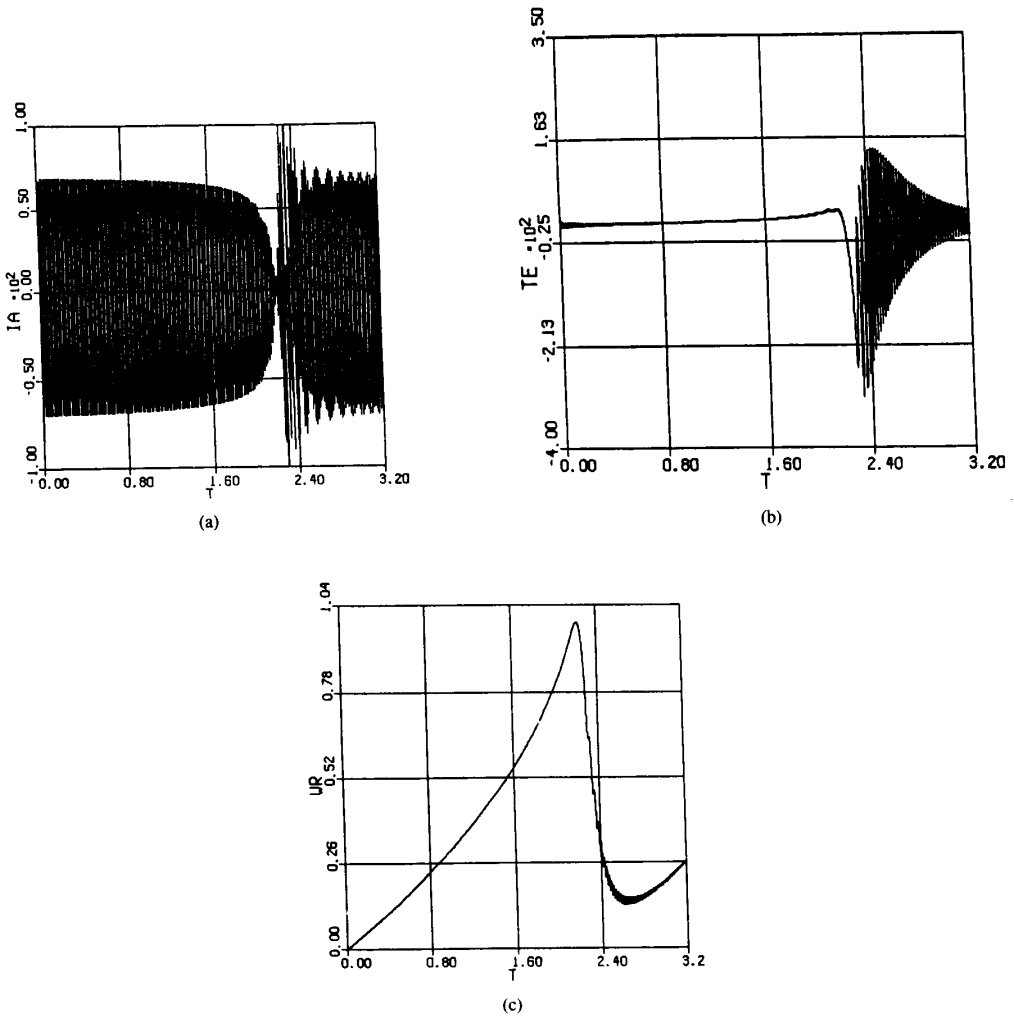

Fig. 11. Starting performance of induction machine fed by series compensated lines. Model with constant parameters. (a) Stator phase *a* current. (b) Runup speed in per unit. (c) Developed electromagnetic torque.

- unsaturated magnetizing reactance per phase, $X_m = 23.30\ \Omega$
- unsaturated stator core reactance per phase, $X_{sc} = 750.0\ \Omega$,
- unsaturated rotor core reactance per phase, $X_{rc} = 1000.0\ \Omega$.

Acknowledgment

The authors wish to thank the Fort Wayne Plant of the General Electric Company for constructing the specially instrumented induction motor.

References

[1] F. P. de Mello and G. W. Walsh, "Reclosing transients in induction motors with terminal capacitors," *IEEE Trans. Power App. Syst.*, vol. PAS-80, pp. 1206–1213, Feb. 1961.

[2] Y. He and T. A. Lipo, "Computer simulation of an induction machine with spatially dependent saturation," *IEEE Trans. Power App. Syst.*, vol. PAS-103, no. 4, pp. 707–714, Apr. 1984.

[3] T. A. Lipo and A. Consoli, "Modeling and simulation of induction motors with saturable leakage reactances," *IEEE Trans. Ind. Appl.*, vol. IA-20, no. 1, pp. 180–189, Jan./Feb. 1984.

[4] J. E. Brown, P. K. Kovacs, and P. Vas, "A method of including the effect of main flux saturation in the generalized equations of ac machines," *IEEE Trans. Power App. Syst.*, vol. PAS-102, pp. 96–103, 1983.

[5] J. A. Melkebeek, "Magnetizing field saturation and dynamic behavior of induction machines; Part I: An improved calculation method for induction machine dynamics," *Proc. Inst. Elec. Eng.*, vol. 130, pt. B, no. 1, pp. 1–9, 1983.

[6] R. S. Ramshaw and G. Xie, "Nonlinear model of nonsalient synchronous machines," *IEEE Trans. Power App. Syst.*, vol. PAS-131, pp. 1809–1815, 1984.

[7] V. Ostovic, "A method for evaluation of transient and steady state performance in saturated squirrel cage induction machines," *IEEE Trans. Energy Conversion*, vol. EC-1, no. 3, pp. 190–192, Sept. 1986.

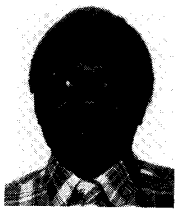

J. O. Ojo (M'87) received the B.Eng. and M.Eng. degrees in electrical engineering from Ahmadu Bello University (ABU), Zaria, Nigeria, in 1977 and 1980, respectively, and the Ph.D. degree from the University of Wisconsin, Madison, in 1987.

He was a Lecturer at ABU from 1978 to 1982 and a Postdoctoral Fellow at the University of Wisconsin, Madison, from 1987 to 1988. Presently, he is an Assistant Professor in the Department of Electrical Engineering at Tennessee Technological University, Cookville, TN. His special interests are energy conversion, control, and power electronics.

Alfio Consoli (M'79–SM'88) was born in Catania, Italy, in 1949. He received the degrees in electrical engineering from the Polytechnic of Turin.

He was an Electrical Engineer in the Research and Development Center of the Fiat, Turin, Italy. In 1975, he joined the Electrical Department of the University of Catania, where he is presently Professor of Electrical Engineering.

He is responsible for the research activities at the University of Catania in the areas of Electromechanical Energy Conversion Systems and Power Electronics. He is also responsible of the graduate-level program for electrical engineering students. He was a Fellow on a NATO Grant at Purdue University and a Visiting Professor at the University of Wisconsin, Madison.

Dr. Consoli is a member of the AEI, and serves on the IAS Industrial Drives Committee.

Thomas A. Lipo (M'64–SM'71–F'87) received the B.E.E. and M.S.E.E. degrees from Marquette University, Milwaukee, WI, in 1962 and 1964, respectively, and the Ph.D. degree in electrical engineering from the University of Wisconsin in 1968. He was an NRC Postdoctoral Fellow at the University of Manchester Institute of Science and Technology, Manchester, England, from 1968 to 1969.

From 1969 to 1979 he was an Electrical Engineer in the Power Electronics Laboratory of Corporate Research and Development of the General Electric Company, Schenectady, NY. He became Professor of Electrical Engineering at Purdue University, Lafayette, IN, in 1979, and later joined the University of Wisconsin, Madison in the same capacity. He has been involved in the research of power electronics and ac drives for over 25 years.

Dr. Lipo has received eleven IEEE prize paper awards including co-recipient of the Best Paper Award in IEEE TRANSACTIONS ON INDUSTRY APPLICATIONS for 1984. In 1986 he received the Outstanding Achievement Award from the IEEE Industry Applications Society for his contributions to the field of ac drives.